JOC The Journal of Organic Chemistry

ARTICLE

pubs.acs.org/joc

Reaction Mechanisms and Structural Characterization of the Reactive Intermediates Observed after the Photolysis of 3-(Hydroxymethyl)benzophenone in Acetonitrile, 2-Propanol, and Neutral and Acidic Aqueous Solutions

Jiani Ma,[†] Ming-De Li,[†] David Lee Phillips,*[,†] and Peter Wan[‡]

[†]Department of Chemistry, The University of Hong Kong, Pokfulam Road, Hong Kong S.A.R., P. R. China

[‡]Department of Chemistry, Box 3065, University of Victoria, Victoria, British Columbia, Canada V8W 3V6

Supporting Information

ABSTRACT: Nanosecond time-resolved resonance Raman (ns-TR^3) spectroscopy was employed to investigate the photoinduced reactions of 3-(hydroxymethyl)benzophenone (**1**) in acetonitrile, 2-propanol, and neutral and acidic aqueous solutions. Density functional theory calculations were utilized to help the interpretation of the experimental spectra. In acetonitrile, the neutral triplet state **1** [denoted here as (*m*-BPOH)^3] was observed on the nanosecond to microsecond time scale. In 2-propanol this triplet state appeared to abstract a hydrogen atom from the solvent molecules to produce the aryphenyl ketyl radical of **1** (denoted here as ArPK of **1**), and then this species underwent a cross-coupling reaction with the dimethylketyl radical (also formed from the hydrogen abstraction reaction) to form a long-lived light absorbing transient species that was tentatively identified to be mainly 2-(4-(hydroxy(3-(hydroxymethyl)phenyl)methylene)cyclohexa-2,5-dienyl)propan-2-ol. In 1:1 H_2O:CH_3CN aqueous solution at neutral pH, (*m*-BPOH)^3 reacted with water to produce the ArPK of **1** and then underwent further reaction to produce a long-lived light absorbing transient species. Three photochemical reactions appeared to take place after 266 nm photolysis of **1** in acidic aqueous solutions, a photoreduction reaction, an overall photohydration reaction, and a novel photoredox reaction. TR^3 experiments in 1:1 H_2O:CH_3CN aqueous solution at pH 2 detected a new triplet biradical species, which is associated with an unusual photoredox reaction. This reaction is observed to be the predominant reaction at pH 2 and seems to face competition from the overall photohydration reaction at pH 0.

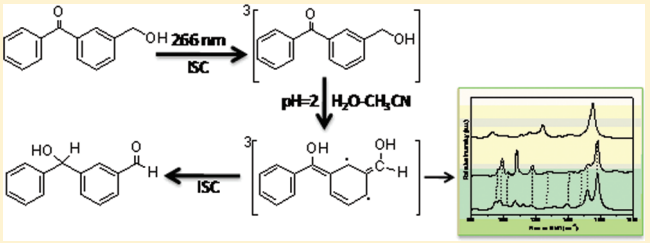

INTRODUCTION

Many benzophenone (BP)-containing compounds have been studied to elucidate their photophysics and photochemistry under a variety of conditions.[1−8] Some commonly observed processes have included Norrish Type I and II reactions and intermolecular hydrogen abstraction reactions as well as photoinduced electron transfer under some conditions.[9−13] Photolysis of a number of BP-containing compounds in organic solvents such as 2-propanol leads to formation of a ketyl radical via hydrogen abstraction from the solvent molecule by the photoexcited ketone species. The ketyl radical can undergo further reactions to produce pinacols or simple reduction of the ketone.[9−13] Recently, Wan and co-workers reported a new kind of photochemical reaction that appears to occur for meta-substituted BP in aqueous solution, in which a formal water-assisted photoredox reaction reduces the ketone to its alcohol and a meta-substituted alcohol moiety is oxidized to its aldehyde (or ketone), while this reaction was not detected for para-substituted derivatives.[14−19] The 3-(hydroxymethyl)benzophenone (**1**) compound was used as a prime example of this new formal water-assisted photoredox reaction. The photochemical reactions of **1** in acidic (pH < 3) aqueous solution was observed to be very efficient with a quantum yield of about 0.6 to produce predominantly 3-formylbenzhydrol (**2**) (95%) and small amounts of 3-formylbenzophenone (**3**) (5%) (see Scheme 1).[15]

Nanosecond transient absorption experiments carried out for **1** in 1:1 H_2O:CH_3CN gave a spectrum composed of two bands (λ_{max} = 325 and 525 nm) that could be attributed to the triplet excited state of the molecule because the triplet state of BP exhibits a similar spectrum.[15] The transient species was found to be quenched by lowering the pH of the aqueous solution, and this suggested that a protonated triplet state could lead to the observed products under acidic conditions. A preliminary mechanism was proposed, and this is displayed in Scheme 2.[15] The mechanism in Scheme 2 indicates that protonation of the excited state of **1** results in formation of an intermediate with a positive charge at the meta position (**4**), similar to an intermediate suggested to be involved in the photodeuteration of 3-methylbenzyophenone[18] and an intermediate suggested by Wirz and co-workers for the acid-catalyzed photohydration of

Received: December 8, 2010
Published: April 05, 2011

Scheme 1. Overall Formal Water-Assisted Photoredox Reaction and Products Produced from Photolysis of 1 in Acidic (pH < 3) Aqueous Solution[15]

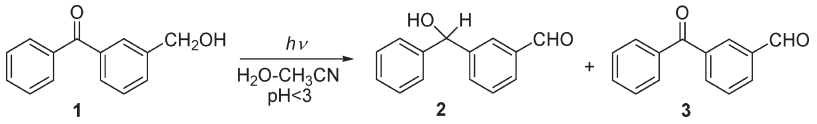

Scheme 2. Preliminary Mechanism Proposed by Wan and Co-workers[15] for the Water-Assisted Photoredox Reaction Seen for 1

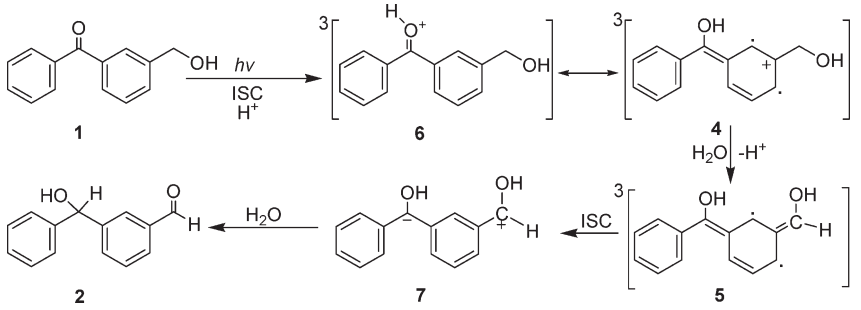

BP.[20] The intermediate **4** then can convert into intermediate **5** that then goes on to form product **2**. The general water-assisted photoredox reaction observed after photolysis of **1** in aqueous acidic conditions, and its reaction mechanism constitute an unusual and important pathway that is different from the typical pathways of BP that are often employed as triplet sensitizers or hydrogen abstractors. This interesting photoredox reaction still needs verification of its mechanism and reactive intermediates. In particular, it is important to obtain some structural characterization of the reactive intermediates to better elucidate the identity and properties of the intermediates and associated reaction mechanism.

When potential reactive intermediates exhibit electronic absorptions in a similar wavelength region and have similar lifetimes, it can be very difficult to clearly identify and distinguish different intermediates from one another by time-resolved absorption spectroscopy methods.[21−25] For reactions where this happens, it is helpful to utilize time-resolved vibrational spectroscopic methods that are able to use the structural information in vibrational frequencies to clearly identify and characterize different intermediates. We have recently used time-resolved resonance Raman (TR^3) spectroscopy to study the photochemistry of BP and BP-containing compounds and obtained new insight into the identity, structure, and properties of different intermediates involved in the reactions of these kinds of molecular systems.[26−30] In this paper, we report TR^3 spectroscopic and density functional theory (DFT) study of the intermediates associated with the reactions after photolysis of **1** in varying solvents. The work here aims to verify the photoredox reaction observed after photolysis of **1** in acidic (pH < 3) aqueous solution by Wan[15] and provides structural information for the reactive intermediates associated with the reaction. To our knowledge, this is the first vibrational spectroscopic characterization of the intermediates observed after photolysis of **1**.

RESULTS AND DISCUSSION

A. Nanosecond TR^3 Spectroscopy of 1 in Acetonitrile (MeCN) and in 2-Propanol Solutions. Figure 1 shows the ns-TR^3 spectra of the intermediates observed after 266 nm photolysis of **1** in MeCN with different delay times indicated near the spectra. Two species were detected in MeCN. The first species has strong Raman bands at 969, 1169, 1227, and 1543 cm^{-1} and is attributed to the neutral triplet state **1** [denoted here as (m-BPOH)^3] mainly due to two reasons. First, the ns-TR^3 spectra of this species exhibit a great similarity with previously observed spectra of the triplet state of BP and

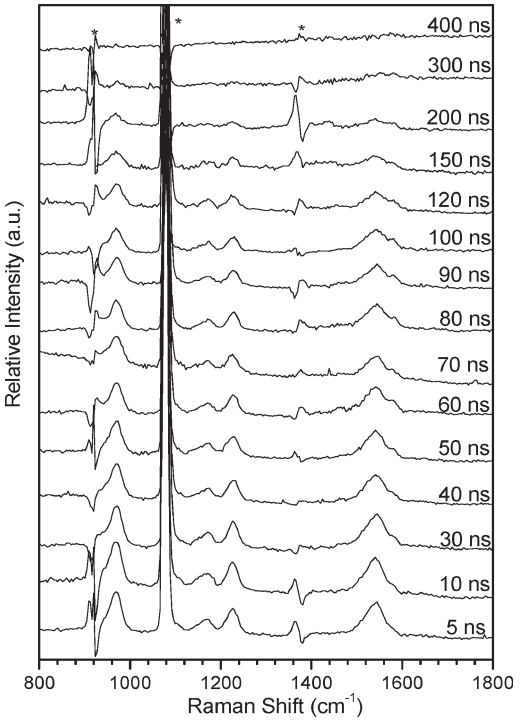

Figure 1. ns-TR^3 spectra of the intermediates observed after 266 nm photolysis of **1** in pure MeCN using a 319.9 nm probe wavelength at various time delays indicated next to the spectra. The asterisks (*) mark regions affected by solvent subtraction artifacts and/or stray light.

dx.doi.org/10.1021/jo1024249 |J. Org. Chem. 2011, 76, 3710–3719

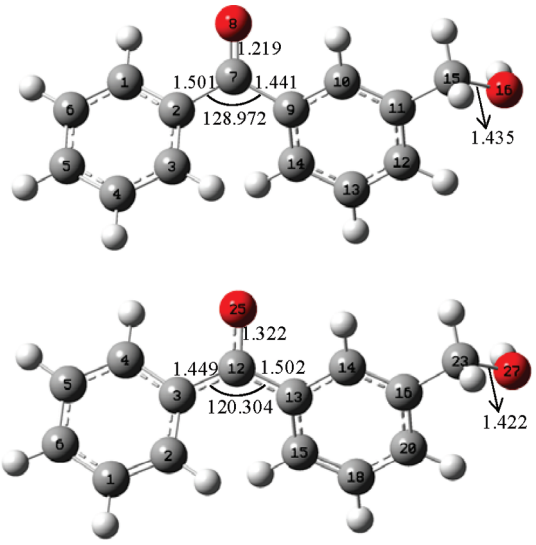

Figure 2. Schematic depiction of the optimized structures of the ground state of **1** (top) and the (*m*-BPOH)^3 (bottom) species obtained from B3LYP/6-311G** DFT calculations. Selected bond lengths (Å) and bond angles (deg) are labeled in the structures.

(*S*)-ketoprofen.[26−30] Second, a comparison between the predicted Raman spectrum from the DFT calculations for the (*m*-BPOH)^3 species and the 5 ns time delay TR^3 spectrum (shown in Figure 2S of the Supporting Information) reveals that the calculated normal Raman spectrum displays reasonably good agreement with the TR^3 spectrum with some differences in the relative intensity patterns that can be attributed to the experimental spectrum being resonantly enhanced while the calculated spectrum is a normal Raman spectrum. Figure 2 displays a simple diagram of the optimized geometry and selected structural parameters obtained from (U)B3LYP/6-311G** calculations for the ground state of **1** and the (*m*-BPOH)^3 species. The time dependence of the intensity of the 1226 cm^{-1} Raman band of (*m*-BPOH)^3 in the ns-TR^3 spectra could be fit with a single exponential function with a decay time constant of ∼113 ns, and a plot of this is shown in Figure 3S of the Supporting Information.

Most of the Raman bands observed from ns-TR^3 spectra of the (*m*-BPOH)^3 intermediate are due to vibrations associated with the ring C−C stretching and C−H bending motions for the 800−1800 cm^{-1} region. For instance, the 1543 cm^{-1} Raman band is mainly due to a ring C−C stretch mode while the 1227 cm^{-1} Raman band is mostly due to the carbonyl C═O stretching mode, and the 969 cm^{-1} Raman feature has contributions mainly from the C−C deformation mode. For aromatic carbonyl compounds, the electronic configuration of the T_1 state determines the T_1 state's reactivity toward the hydrogen abstraction reaction with hydrogen donor reagents.[31−36] In general, a T_1 state with mainly n−π^* character will have a high efficiency for hydrogen abstraction reaction, but a triplet state with a π−π^* character has little if any reactivity for the hydrogen abstraction reaction. Previous studies determined that the frequency of the C−O stretch mode appears in the 1400−1600 cm^{-1} range for a π−π^* character triplet state and in the 1200−1400 cm^{-1} region for a typical n−π^* character triplet state. The C−O stretching frequency for (*m*-BPOH)^3 was seen at 1236 cm^{-1}, and this indicates that (*m*-BPOH)^3 has n−π^* character. Therefore, a high efficiency for hydrogen abstraction reaction in certain solvents is expected. Another species that has a characteristic Raman band at

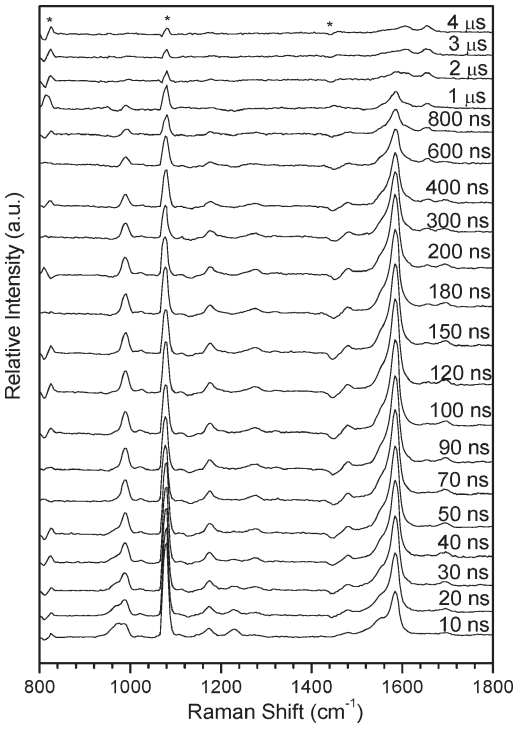

Figure 3. ns-TR^3 spectra observed after 266 nm photolysis of **1** in 2-propanol solution using a 319.9 nm probe wavelength at various time delays indicated next to the spectra. The asterisks (*) mark regions affected by solvent subtraction artifacts and/or stray light.

1584 cm^{-1} was also observed after 10 ns. Clear identification of this species at 1584 cm^{-1} is difficult because of the weak intensity of the only clear fingerprint band and will not be considered further here.

Figure 3 displays the ns-TR^3 spectra of intermediates observed after 266 nm photolysis of **1** in 2-propanol solution at various time delays. The first species appearing at early times has its most intense bands at 967, 1229, and 1546 cm^{-1} and is assigned to (*m*-BPOH)^3 on account of the very high similarity of the 5 ns spectrum from Figure 3 to the (*m*-BPOH)^3 spectrum recorded in MeCN (see Figure 1). As the (*m*-BPOH)^3 Raman signal is quenched, a new species with Raman bands at 989, 1176, 1481, 1584, and 1697 cm^{-1} is observed in Figure 3. Because 2-propanol is a strong hydrogen donor solvent, (*m*-BPOH)^3 can easily abstract a hydrogen atom from 2-propanol to produce an arylphenyl ketyl radical (denoted hereafter as ArPK of **1**), and the second species in the TR^3 spectra is tentatively attributed to the ArPK of **1** species. Figure 4 displays a comparison of the TR^3 spectrum obtained at the time delay of 90 ns (top) selected from Figure 3 with the DFT-calculated Raman spectrum (bottom) for the ArPK of **1** intermediate with its structure displayed near the top of the spectrum. The DFT-calculated Raman spectrum for the ArPK of **1** intermediate is in good agreement with the ns-TR^3 spectrum in Figure 4. The Raman band at 987 cm^{-1} in Figure 3 for the ArPK of **1** intermediate was fit with a Lorentzian band shape to obtain the time dependence of this species, and the kinetic obtained is displayed in Figure 4S of the Supporting Information. Under the experimental conditions employed here, the ArPK of **1** intermediate had a growth time constant of ∼36 ns and a decay time constant of ∼614 ns.

dx.doi.org/10.1021/jo1024249 |*J. Org. Chem.* 2011, 76, 3710–3719

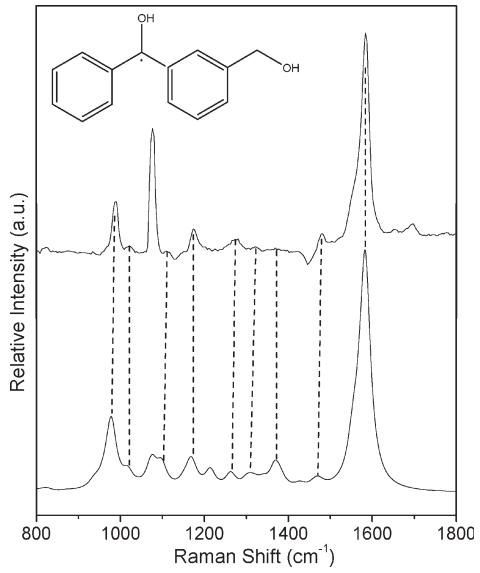

Figure 4. Comparison of the ns-TR^3 spectrum of the ArPK of **1** radical species acquired at 90 ns time delay after photolysis of **1** in 2-propanol solution (top) to the calculated normal Raman spectrum (bottom) of the ArPK of **1** species with the schematic structure shown in the top of the figure.

Besides (*m*-BPOH)^3 and ArPK of **1** intermediates, a third species appeared at 1654 cm^{-1} at longer time delays in Figure 3. The hydrogen abstraction reaction produces both a dimethyl ketyl (DMK) radical and an ArPK of **1** radical. Previous studies of BP[29] and its derivatives in 2-propanol have observed that the ArPK radical species can cross-couple with the DMK radical mainly at the para-position to form a long-lived light-absorbing transient species (LAT). Similarly, the third species seen in Figure 3 can be attributed mostly to the *p*-ArPK−DMK of **1** intermediate. Figure 5S of the Supporting Information displays a comparison of the experimental ns-TR^3 spectrum at 10 μs (top) obtained from ns-TR^3 in 2-propanol to the calculated spectrum for the *p*-ArPK−DMK of **1** species (bottom) with its structure shown next to the spectrum. Inspection of Figure 5S shows that the calculated *p*-ArPK−DMK of **1** normal Raman spectrum exhibits reasonable agreement with the experimental TR^3 spectrum and supports the assignment of the third species to the *p*-ArPK−DMK of **1** intermediate.

Time-dependent density functional theory (TD-DFT) calculations were also done for the ArPK of **1** species, and these results are displayed in Table 1S of the Supporting Information. The calculations predict that the ArPK of **1** species has an intense electronic transition at 325 nm which is close to the probe wavelength used in the ns-TR^3 experiments, and this is consistent with the high intensity of the Raman bands of the ArPK of **1** intermediate in the ns-TR^3 spectra.

B. Nanosecond TR^3 Spectroscopy of 1 in Neutral and Acidic Aqueous Solutions. Figure 5 displays the ns-TR^3 spectra acquired after photolysis of **1** in neutral aqueous solution (MeCN:H_2O, 1:1) at different time delays. Like the ns-TR^3 spectra obtained in 2-propanol solution, three species are observed in the ns-TR^3 spectra shown in Figure 5. The spectra of the first species in Figure 5 with intense Raman bands at 969, 1169, 1227, and 1543 cm^{-1} are very similar to the spectra observed for the (*m*-BPOH)^3 species seen in MeCN and 2-propanol solutions (see Figures 1 and 3) and can be attributed to the (*m*-BPOH)^3

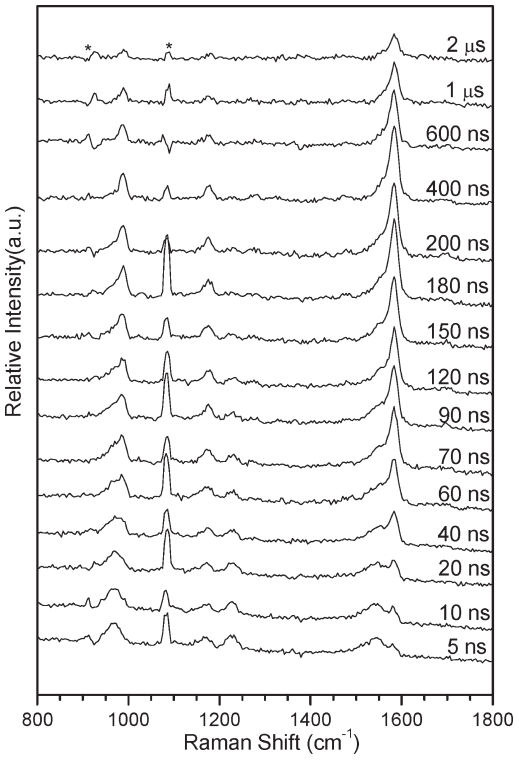

Figure 5. ns-TR^3 spectra of the intermediates observed after 266 nm photolysis of **1** in neutral aqueous solution (MeCN:H_2O, 1:1) obtained using a 319.9 nm probe wavelength at various time delays indicated next to the spectra. The asterisks (*) mark regions affected by solvent subtraction artifacts and/or stray light.

Scheme 3. Reaction Mechanism Proposed by Wirz and Co-workers for the Photohydration of BP in Acidic Aqueous Solutions[20]

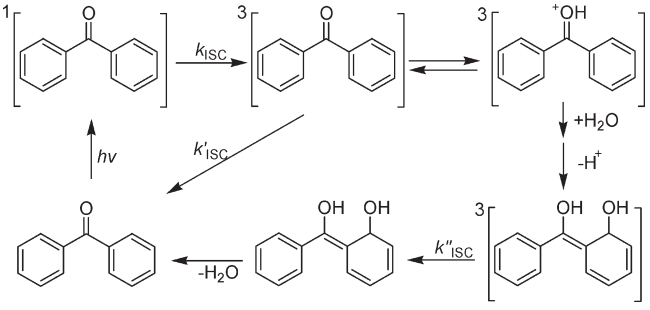

intermediate and/or the closely related protonated form of this intermediate (see Scheme 3 for the equilibrium between these species). The spectra of the second species with its intense bands at 988, 1177, 1273, 1478, 1582, and 1696 cm^{-1} are very similar to the spectra observed for the ArPK of **1** radical seen in the 2-propanol solution (see Figure 3) and can similarly be attributed to the ArPK of **1** radical. The comparison of ns-TR^3 spectrum acquired at 600 ns after photolysis of **1** in 1:1 MeCN:H_2O solvent with that of **1** in neat 2-propanol acquired at 600 ns shows fairly good agreement in the Raman shift frequencies. This suggests that the second species observed in the neutral aqueous solution is the ArPK of **1** intermediate. This ArPK of **1** radical observed in water could be produced by an analogous hydrogen

dx.doi.org/10.1021/jo1024249 |*J. Org. Chem.* 2011, 76, 3710–3719

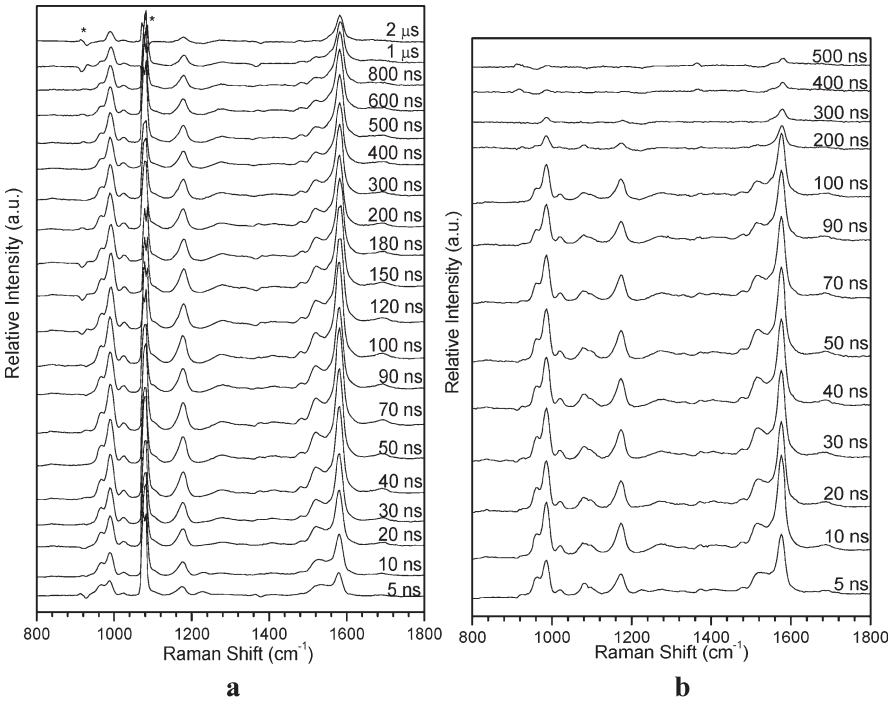

Figure 6. ns-TR^3 spectra of intermediates obtained after 266 nm photolysis of ~3×10^{-4} M **1** in an acidic (pH = 2) aqueous solution (MeCN:H_2O, 1:1) in open air (a) and oxygen-purging conditions (b) obtained using a 319.9 nm probe wavelength at various time delays indicated next to the spectra. The asterisks (*) marks regions affected by solvent subtraction artifacts and/or stray light.

abstraction reaction from water which is abundant in the aqueous system; however, this may not be easy because this is probably a very endergonic process for water (about ΔG = +85 kJ/mol and ΔH = +28 kJ/mol for BP based on data from references 37 and 38). It is useful to note that photohydration reaction was observed for BP in acidic aqueous solutions by Wirz and co-workers[20] (see the proposed mechanism in Scheme 3 for the photohydration of BP in water) so this may also be occurring in aqueous environments for the system of interest here. Examination of Scheme 3 shows that the (*m*-BPOH)^3 intermediate is in equilibrium with its protonated form. It is conceivable that hydrated electrons present in the aqueous solution could react with the protonated form of the (*m*-BPOH)^3 intermediate to form the ArPK of **1** radical. The protonation of the triplet state BP was observed to be very fast for BP (on the order of several hundred picoseconds), and the hydrated electron was also observed on the hundreds of picoseconds to one or two nanoseconds in acidic aqueous solutions.[20] A fast two-step process (e.g., protonation of the (*m*-BPOH)^3 intermediate followed by reaction with an hydrated electron) could possibly lead to apparent fast conversion of the (*m*-BPOH)^3 intermediate into the ArPK of **1** radical as observed in the ns-TR^3 spectra of Figure 5 after photolysis of **1** in neutral aqueous solution (MeCN:H_2O, 1:1). At present, it is not clear which possible mechanism is mainly responsible for the production of the ArPK of **1** radical in neutral aqueous solutions, and further experimental and theoretical work is needed to better understand the complex interplay between different reaction pathways in neutral aqueous solutions. The third species seen in Figure 5 appears at long time delays and can be tentatively assigned to some sort of LAT species formed from some reaction of the ArPK of **1** radical with water or other intermediate present in the solution. Because the signal of the third species in the TR^3 spectra is relatively weak, we shall not attempt to make a definitive assignment here.

Figure 6a shows the ns-TR^3 spectra of intermediates obtained after 266 nm photolysis of **1** in an acidic (pH = 2) aqueous solution (MeCN:H_2O, 1:1). The photochemical behavior of **1** under this condition is obviously different from that for the analogous experiments done in neutral aqueous solution. In Figure 6a new Raman bands appear at 962 and 1518 cm^{-1}. Since the difference between the experiments done in pH = 2 MeCN:H_2O (1:1) and neutral aqueous solutions is the acid concentration, the new species may result from a reaction catalyzed by the presence of the acid in aqueous solutions. In order to study a possible acid catalysis effect, ns-TR^3 experiments were also conducted in acidic aqueous solutions at the pH values of 4 and 0, and their ns-TR^3 spectra are presented in Figure 7. There are at least three photochemical reactions that appear to occur for the 266 nm photolysis of **1** in acidic aqueous solutions. The first type of reaction is the photoreduction reaction that was the predominant reaction observed for analogous experiments performed in neutral aqueous solutions. In acid aqueous solutions, the intensity of the ArPK of **1** radical Raman bands is much smaller than that in the neutral solution[27] so the probable contribution from this photoreduction reaction to the ns-TR^3 spectra obtained under acidic aqueous conditions can be considered to be small. An overall photohydration reaction may also take place in moderate acidic aqueous solution similar to the photohydration reaction observed for BP in acidic aqueous solutions by Wirz and co-workers[20] so this may be a second type of reaction that may be seen in the spectra of Figures 6 and 7. Scheme 3 shows the proposed reaction mechanism for the photohydration of BP in acidic aqueous conditions.[20] The photoredox reaction reported by Wan and co-workers for the photolysis of **1** in acidic solutions is a third type of reaction that may be seen in the spectra of Figures 6 and 7.

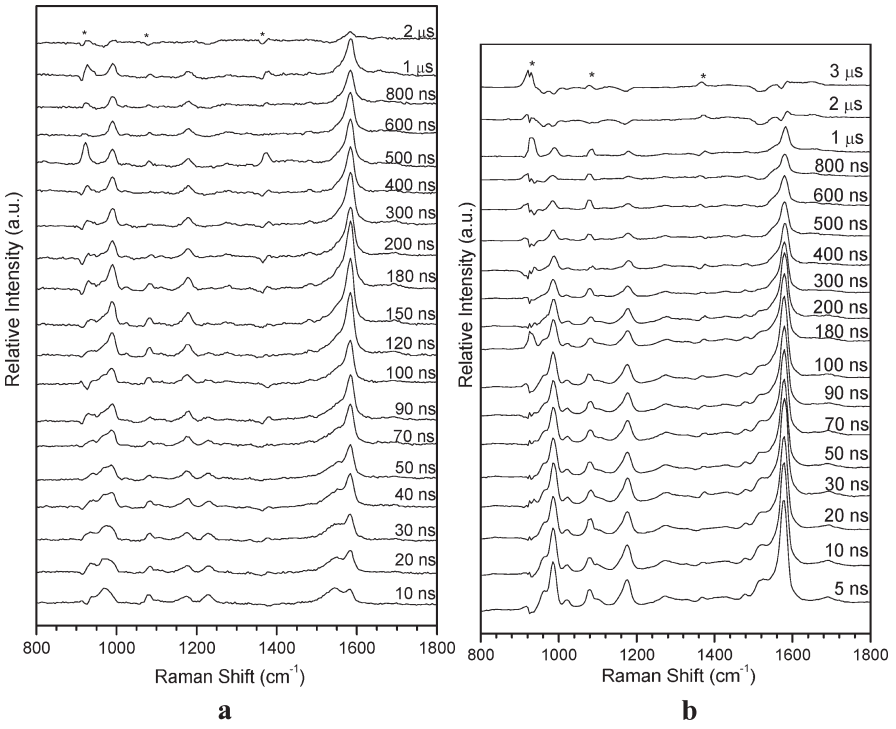

Figure 7. The 319.9 nm probe wavelength ns-TR[3] spectra of intermediates obtained after 266 nm photolysis of ~3×10^{-4} M **1** in an acidic aqueous solution (MeCN:H_2O, 1:1) with pH = 4 (a) and pH = 0 (b) conditions at various time delays indicated next to the spectra. The asterisks (*) mark regions affected by solvent subtraction artifacts and/or stray light.

Comparison of the spectra shown in Figures 6 and 7 demonstrates that under pH = 0 and 2 conditions the intensity of the Raman band at 1584 cm^{-1} is stronger than that under pH = 4 conditions. The spectra at 5 ns delay time in the pH = 2 and pH = 0 aqueous solutions suggest that the Raman band at 1584 cm^{-1} has higher intensity in the pH = 0 solution. On the other hand, the intensities of the new Raman bands at 962 and 1518 cm^{-1} are much stronger in the pH = 2 aqueous solution than in the pH = 4 and pH = 0 solutions. According to the study of Wirz and co-workers, the efficiency of the photohydration of BP in acidic aqueous solutions reached a maximum at the pH value of 0.[21] On the basis of the preceding results, the strong Raman band at 1584 cm^{-1} may have contributions from transient species associated with both the photoredox reaction and the photoreduction reaction leading to the overall photohydration reaction, while the Raman bands at 962 and 1518 cm^{-1} probably have mainly contributions from intermediates involved in the photoredox reaction. Because we could not adequately sort out the different contributions from the two reactions to the Raman band at 1584 cm^{-1}, a quantitative estimate of the rate constant for the photohydration reaction and the photoredox reaction is not given here.

The signal associated with the photoredox reaction could also be detected in the pH = 4 acid aqueous solution. Analysis of the spectra shown in Figure 7a shows that in the pH = 4 aqueous solution the relative intensity of the Raman bands at 962 and 1518 cm^{-1} were apparently lower than that in the pH = 2 solution, which indicates that the photoredox reaction is not so favorable in the pH = 4 aqueous solution as that in the pH = 2 aqueous solution. Because the photoredox reaction of **1** in acidic aqueous solution is thought to be acid-catalyzed one would expect a higher reaction conversion under more acidic conditions. Wan and co-workers[15] also mentioned that decreasing the pH value gave a higher yield of 3-formylbenzhydrol, the final product of the photoredox reaction consistent with the above trend of the intensity of the Raman bands at 962 and 1518 cm^{-1} associated with a reactive intermediate leading to the photoredox products. A later study[19] reported that the photoredox reaction was not obvious in very high acidic aqueous solutions with pH = 0 and below. Examination of spectra in Figure 7b suggests that the photoredox reaction can still be observed in a pH = 0 aqueous solution but the efficiency of the photoredox reaction was markedly decreased compared to that in the pH = 2 aqueous solution using the criterion of the Raman features at 962 and 1518 cm^{-1} as marker bands for the photoredox reaction. The relative intensities of these marker bands as a function of pH of the acidic aqueous solutions indicate there may be significant competition from some side reactions in pH = 0, which is probably the photohydration reaction. Inspection of Scheme 3 suggests that the protonation of the carbonyl oxygen is an integral part in the photohydration reaction of BP in acidic aqueous solution. As mentioned previously, the efficiency of the photohydration reaction in acid aqueous solutions appears to reach a maximum at a pH value of 0. If the photohydration reaction is more favorable than the photoredox reaction in a pH = 0 aqueous solution, the efficiency of the photoredox reaction will become decreased relative to the corresponding reaction in pH = 2 aqueous solution. This seems consistent with our present results and previous observations of Wirz and co-workers[20] for BP and Wan and co-workers[15,19] for **1** in acidic aqueous solutions.

There are four intermediate species involved in the proposed mechanism by Wan and co-workers for the photoredox reaction of **1** after photolysis in acidic aqueous solutions. It is necessary to

dx.doi.org/10.1021/jo1024249 |*J. Org. Chem.* 2011, 76, 3710–3719

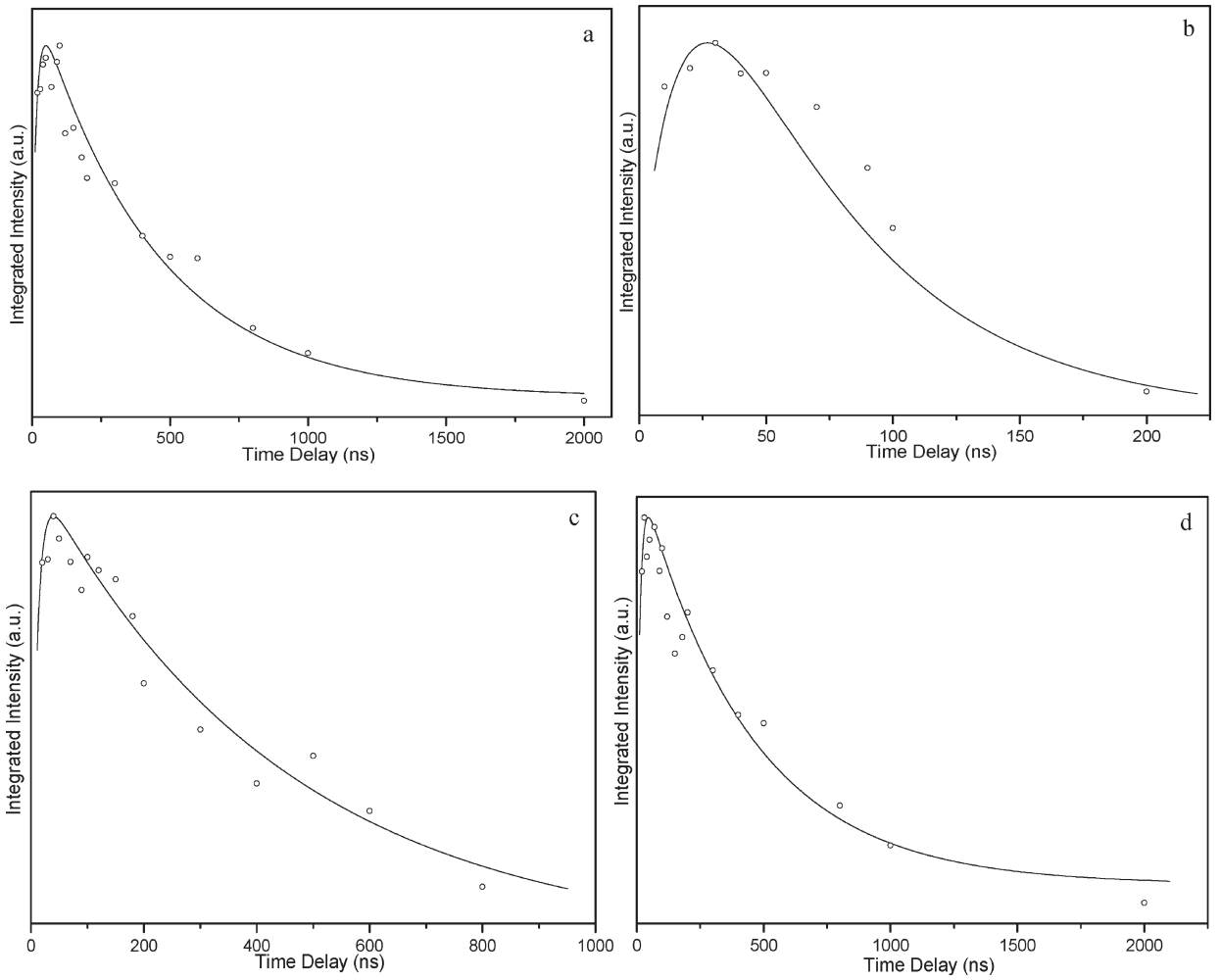

Figure 8. Time dependence of the 962 cm^{-1} Raman band of the species related to the photoredox reaction obtained in the ns-TR^3 measurements with (a) ~3×10^{-4} M of **1** in open air, (b) ~3×10^{-4} M of **1** with oxygen purging (with ~18 ns growth time constant and ~60 ns decay time constant), (c) ~6×10^{-4} M of **1**, (d) ~9×10^{-4} M of **1** in pH = 2 MeCN:H_2O (1:1) fit with a two-exponential function. See text for more details.

determine which species appear in the ns-TR^3 spectra under acidic aqueous conditions and are associated with the photoredox reaction. To study the quenching effect by oxygen, ns-TR^3 experiments were also performed with oxygen being bubbled through the sample solution, and these spectra are displayed in Figure 6b. Plots of the integrated areas for the new species using a marker band at 962 cm^{-1} as a function of time delay were obtained in both open air condition and oxygen bubbling condition and shown in Figure 8a,b. The lifetime of this species in the oxygen-purging experiment is ~60 ns, which is obviously shorter than that under the corresponding open air conditions with a lifetime of ~430 ns. This suggests that this new species observed in acidic aqueous solutions has some triplet character, which would be likely associated with intermediates **4** or **5** in Scheme 2 rather than with species **7**.

The DFT calculations for the species **4** and **5** were performed and compared with the spectrum of the new species observed in the ns-TR^3 experiments performed under conditions associated with the observation of the intriguing photoredox reaction. The spectrum obtained in the pH = 2 aqueous solution at 120 ns time delay from Figure 6a was selected as being diagnostic of the intermediate leading to the photoredox product. A comparison of this experimental spectrum to the calculated Raman spectra for the species **4** and **5** is shown in Figure 9. Inspection of Figure 9 suggested that the new intermediate species observed in moderately acidic aqueous solutions shows more similarity with the species **5** than with the species **4**. This reasonable agreement between the TR^3 spectrum of the new intermediate species (middle spectrum of Figure 9) and the DFT calculated normal Raman spectrum of the intermediate **5** (bottom spectrum of Figure 9) and the triplet character deduced from the oxygen quenching experiment leads us to attribute this new species (this is associated with the photoredox reaction) to the triplet biradical intermediate **5**. Results from TD-DFT (UB3LYP/6-311G**) calculations for the intermediate species **4** and **5** provide further support for this assignment. These computational results are displayed in Table 2S of the Supporting Information, and the absorption spectra deduced from the calculations are shown in Figure 7S of the Supporting Information. Examination of the computational results indicates that the triplet biradical species **5** has a higher oscillator strength near the probe laser wavelength (319.9 nm) used in the ns-TR^3 experiments whereas the predicted transient absorption spectrum of **4** displays a relatively weak oscillator strength near the 319.9 nm probe laser wavelength. In this case, the species **4** may not easily be detected in the ns-TR^3 experiments with a 319.9 nm probe wavelength because it has a very

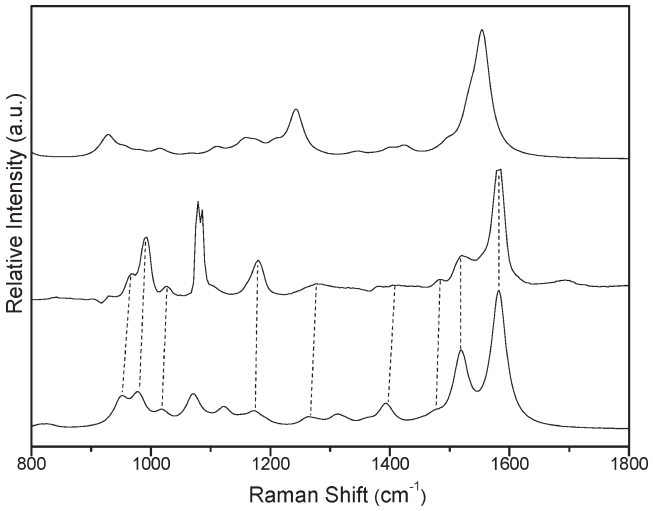

Figure 9. The spectrum obtained in the pH = 2 aqueous solution at 120 ns time delay from Figure 7a was selected as being diagnostic of the intermediate leading to the photoredox reaction. A comparison of this experimental spectrum (middle) to those calculated normal Raman spectra of species **4** (top) and **5** (bottom) is shown.

Table 1. Dynamics of the Intermediate Species 5 Obtained in pH = 2 Aqueous Solutions (MeCN:H_2O, 1:1) with Different Concentrations of 1 (see text for details)

concentration of **1** (M)	growth time constant (ns)	decay time constant (ns)
3×10^{-4}	16	430
6×10^{-4}	10	440
9×10^{-4}	10	430

small Raman signal due to its weak resonance enhancement. Thus, the species observed in our ns-TR^3 spectra in pH = 2 acid aqueous solution is most consistent with and assigned to the triplet biradical intermediate species **5** (see Scheme 2).[15]

The effect of the substrate concentration on the resulting photochemical behavior of **1** was studied. Ns-TR^3 experiments were done for the 266 nm photolysis of **1** with the concentrations of ~6×10^{-4} M and ~9×10^{-4} M in pH = 2 aqueous solutions, and these spectra are shown in Figure 6S of the Supporting Information. The Raman band area at 962 cm^{-1} was integrated, and the corresponding kinetic is shown in Figure 8c,d. The respective growth time constant and decay time constant for the intermediate **5** species with concentrations of ~3×10^{-4} M, ~6×10^{-4} M, and ~9×10^{-4} M in pH = 2 aqueous solutions are given in Table 1. This is consistent with the study by Wan that the photoredox reaction was unaffected by dilution and was observed down to the lowest concentration of ~10^{-6} M of **1**.[15] The lack of a strong concentration dependence on the lifetime constant upon the concentration of **1** suggests that we are mainly observing the photoredox reaction that does not involve diffusional encounters with other molecules of **1** in moderately acidic aqueous solutions. The isotopic effect experiments in D_2O/CH_3CN conducted found that no benzhydrol proton was observed.[19] This result also demonstrated that the methine proton of the final product of the photoredox reaction arises from water rather than from the substrate molecule. Consequently, the hydrogen migration in the photoredox reaction was attributed to a water-assisted process. This suggests that the photoredox reaction is assisted by the water molecules and does not involve diffusional encounters with other molecules of **1**.

We did not observe obvious Raman bands for the product 3-formylbenzhydrol in the 319.9 nm probe ns-TR^3 experiments under the experimental conditions, which is anticipated because the probe wavelength of 319.9 nm used in our experiments may not be a suitable wavelength for probing the signal of 3-formylbenzhydrol. TD-DFT calculation results for 3-formylbenzhydrol are shown in Table 3S of the Supporting Information, and these results indicate that there is very little absorption for 3-formylbenzhydrol at 336 nm which is near the probe wavelength used in the ns-TR^3 experiments. This is consistent with not observing any Raman signal of 3-formylbenzhydrol in the 319.9 nm probe ns-TR^3 experiments on account it does not have appreciable absorption at 319.9 nm.

CONCLUSION

Our TR^3 study here observed formation of the neutral triplet state **1** [denoted as $(m\text{-BPOH})^3$] on the nanosecond to microsecond time scale in acetonitrile. In the strong hydrogen donor solvent, 2-propanol, $(m\text{-BPOH})^3$ abstracted a hydrogen atom from the solvent molecule to form the arylketyl radical of **1** (denoted as ArPK of **1**) and then reacted via a cross-coupling reaction with the dimethylketyl (DMK) radical (also formed from the hydrogen abstraction reaction) to produce a long-lived light absorbing transient (LAT) species 2-(4-(hydroxy(3-(hydroxymethyl)phenyl)methylene) cyclohexa-2,5-dienyl)propan-2-ol that was denoted as *p*-ArPK—DMK of **1**. In 1:1 H_2O:CH_3CN aqueous solution at near neutral pH, the $(m\text{-BPOH})^3$ species appeared to react in some way to produce the ArPK of **1** that underwent further reaction to produce a longer lived intermediate. Three photochemical reactions appeared to occur for the 266 nm photolysis of **1** in acidic aqueous solutions, the photoreduction reaction, an overall photohydration reaction, and an unusual photoredox reaction. When the TR^3 experiments were performed in 1:1 H_2O:CH_3CN acidic aqueous solution at pH 2, the photoredox reaction appeared to be the predominant one. This is consistent with the reported results of Wan that 3-formylbenzhydrol (**2**) was observed with a high quantum yield of about 0.6 from the photoredox reaction under similar conditions.[15] A new intermediate in TR^3 experiments in 1:1 H_2O:CH_3CN acidic aqueous solution at pH 2 with Raman bands at 962 and 1518 cm^{-1} is associated with the photoredox reaction and is identified as the triplet biradical species **5** from comparison of the TR^3 spectra to the predicted Raman spectrum of **5** from DFT calculations and oxygen-quenching experiments. The lack of significant substrate concentration dependence on the growth and decay times of species **5** indicates that the photoredox reaction is mainly a water-assisted process which does not involve diffusional encounters with other molecules of **1**. The photoredox reaction appears to experience some competition from the overall photohydration reaction in aqueous solution at pH 0.

EXPERIMENTAL AND COMPUTATIONAL METHODS

The 3-(hydroxymethyl)benzophenone (*m*-BPOH) compound was synthesized following the methods detailed previously in the literature,[16] and the basic route is also shown in Scheme 1S of the Supporting Information. Briefly, the first synthesis step combined 3-methylbenzophenone with 1.2 equiv of *N*-bromosuccinimide and a catalytic amount of benzoyl peroxide in 50 mL of benzene solvent. This reaction mixture

was refluxed for 14 h, and then the mixture was washed twice with 25 mL of distilled water and subsequently dried with anhydrous $MgSO_4$. The solvent was then removed in vacuum. The crude 3-benzoylbenzyl bromide was then combined with 5 equiv of $CaCO_3$ in a 100 mL of H_2O:dioxane (1:1, V:V) solution and then refluxed for 17 h. After conventional purification, the *m*-BPOH was obtained utilizing chromatography (silica gel, 1:1 ethyl acetate−hexane). The purity of the *m*-BPOH sample from the ^{1}H NMR spectra was estimated to be greater than 97%. ^{1}H NMR (400 MHz, $CDCl_3$) δ: 7.81−7.79 (m, 3H), 7.73−7.72 (d, 1H), 7.63−7.58 (m, 2H), 7.51−7.47 (m, 3H), 4.77 (s, 2H), 1.62 (s, 1H).

Spectroscopic grade acetonitrile (MeCN), isopropyl alcohol (IPA), perchloric acid ($HClO_4$), and deionized water were used as solvents for the experiments reported here. Unless noted, the sample solutions of *m*-BPOH employed in the ns-TR^3 experiments in MeCN, IPA, and mixed solvents were all with the concentration of $\sim 3 \times 10^{-4}$ M. All of the mixed solvent ratios are of volume ratio. There were four sets of sample solutions in 1:1 MeCN:H_2O with final pH values of 0, 2, 4, and 7 using $HClO_4$ to adjust the pH value as needed.

UV−vis experiments were done to determine reasonable pump and probe excitation wavelengths used in the nanosecond time-resolved resonance Raman (ns-TR^3) experiments. Figure 1S displays the UV−vis spectrum of *m*-BPOH in MeCN with the 266 nm pump and 319.9 nm probe wavelengths used in the ns-TR^3 experiments indicated above the spectrum. Ns-TR^3 experiments were performed using an experimental apparatus and method described previously in our laboratory,[26−30,36] and only a brief description is given here. The fourth harmonic of a Nd:YAG nanosecond pulsed laser supplied the 266 nm pump wavelength and the third anti-Stokes hydrogen Raman-shifted laser line from the second harmonic of a second Nd:YAG laser supplied the 319.9 nm probe wavelength used in the ns-TR^3 experiments. The 266 nm pump pulse excited the sample to initiate the photochemical reactions and the 319.9 nm probe pulse interrogated the sample and the intermediate species produced by the pump pulse. The laser beams were lightly focused and aligned so that they were overlapped onto a flowing liquid stream of sample. The diameter of the pump beam was adjusted to be slightly larger than that of the probe beam at the overlapping volume in the liquid jet in order to minimize the ground-state normal Raman signal. A pulse delay generator was employed to electronically control the time delay between the pump and probe laser beams from the two different Nd:YAG lasers operated at a repetition rate of 10 Hz. The Raman scattered light was acquired using a backscattering geometry and then detected by a liquid nitrogen-cooled charge-coupled device (CCD) detector. The TR^3 signal was acquired for 10 s by the CCD before being read out to an interfaced PC computer, and 10 scans of the signal were accumulated to produce a resonance Raman spectrum. The ns-TR^3 spectra presented in this paper were obtained from subtraction of an appropriately scaled probe-before-pump spectrum from the corresponding pump−probe resonance Raman spectrum to remove nontransient bands. Pure MeCN Raman bands were employed to calibrate the Raman shifts of the ns-TR^3 spectra with an estimated accuracy of 5 cm^{-1}. A Lorentzian function was used to integrate the Raman bands of the species of interest in the ns-TR^3 spectra in order to determine their areas and elucidate the growth and decay time constants of the species observed in the experiments.

In order to assist the assignments for the vibrational bands of the intermediate species observed in the ns-TR^3 experiments, density functional theory (DFT) calculations were done (employing (U)B3LYP method with a 6-311G** basis set) to determine the optimized geometries and vibrational wavenumbers for all of the likely species that may be potential intermediates associated with the photochemical reaction of **1**. No imaginary frequencies were observed at any of the optimized structures studied here. A Lorentzian function with a 15 cm^{-1} bandwidth was used for the Raman vibrational frequencies and the relative intensities to obtain the computational Raman spectra that were compared to the experimental TR^3 spectra. A frequency scaling factor of 0.974 was used in the comparison of the calculated results with the experimental spectra. All the calculations presented in this paper were performed using the Gaussian 03[39] program suite installed on the High Performance Computing cluster at the Computer Centre in The University of Hong Kong.

■ ASSOCIATED CONTENT

Supporting Information. Figure 1S presents UV−vis absorption spectra of **1** in pure MeCN, Figure 2S shows comparison of the experimental ns-TR^3 spectrum of the first species observed in MeCN at 5 ns time delay to the calculated normal Raman spectrum of (*m*-BPOH)^3, Figure 3S shows the time dependence of the 1226 cm^{-1} Raman band of ^{3}(*m*-BPOH) obtained from ns-TR^3 measurements in MeCN, Figure 4S shows the time dependence of the 987 cm^{-1} Raman band of the ArPK of **1** obtained in the ns-TR^3 measurements in 2-propanol, Figure 5S shows the comparison of the experimental TR^3 spectrum at 10 μs obtained from the ns-TR^3 spectra in 2-propanol solution to the calculated spectrum for the *p*-ArPK−DMK of **1** species, Figure 6S shows ns-TR^3 spectra of $\sim 6 \times 10^{-4}$ M and $\sim 9 \times 10^{-4}$ M of intermediates observed after 266 nm photolysis of **1** in a pH = 2 MeCN:H_2O (1:1) solution. Tables 1S, 2S, and 3S show the excited state energies and oscillator strengths from TD-DFT calculations for the ArPK of **1** radical, the transient species **4** and **5**, and the final product of the photoredox reaction 3-formylbenzhydrol (**2**). Cartesian coordinates, total energies, and vibrational zero-point energies for the optimized geometry from the (U)B3LYP/6-311G** calculations for the compounds and intermediates considered in this paper are given. This material is available free of charge via the Internet at http://pubs.acs.org.

■ AUTHOR INFORMATION

Corresponding Author

*E-mail: phillips@hku.hk; tel: 852-2859-2160; fax: 852-2957-1586

■ ACKNOWLEDGMENT

The research was supported by grants from the Research Grants Council of Hong Kong (HKU 7035/08P) to D.L.P. D.L.P. thanks the Croucher Foundation for the Award of a Senior Research Fellowship and the University of Hong Kong for the Outstanding Researcher Award. Support from the University Grants Committee Areas of Excellence Scheme (AoE/P-03/08) and the Special Equipment Grant (SEG HKU/07) is also gratefully acknowledged.

■ REFERENCES

(1) Moore, W. M.; Hammond, G. S.; Foss, R. P. *J. Am. Chem. Soc.* **1961**, *83*, 2789–2794.
(2) Costa, C. V.; Grela, M. A.; Churio, M. S. *J. Photochem. Photobiol., A* **1996**, *99*, 51–56.
(3) Yoshihisa, M.; Yoshizumi, K.; Kinichi, O. *J. Phys. Chem.* **1992**, *96*, 6566–6570.
(4) Bhasikuttan, A. C.; Singh, A. K.; Palit, D. K.; Sapre, A. V.; Mittal, J. P. *J. Phys. Chem. A* **1998**, *102*, 3470–3480.
(5) Miyasaka, H.; Mataag, N. *Bull. Chem. Soc. Jpn.* **1990**, *63*, 131–137.
(6) Singh, A. K.; Palit, D. K.; Mukherjee, T. *J. Phys. Chem. A* **2002**, *106*, 6084–6093.
(7) Shah, B. K.; Rodgers, M. A. J.; Necker, D. C. *J. Phys.Chem. A* **2004**, *108*, 6087–6089.

(8) (a) Matinez, L. J.; Scaiano, J. C. *J. Am. Chem. Soc.* **1997**, *119*, 11066–11070. (b) Laferrière, M.; Sanrame, C. N.; Scaiano, J. C. *Org. Lett.* **2004**, *6*, 873–875. (c) Lukeman, M.; Scaiano, J. C. *J. Am. Chem. Soc.* **2005**, *127*, 7698–7699.
(9) Sakamoto, M.; Cai, X. C.; Kim, S. S.; Fujitsuka, M.; Majima, T. *J. Phys. Chem. A* **2007**, *111*, 223–229.
(10) Scaiano, J. C. *J. Photochem.* **1973−1974**, *2*, 81–118.
(11) Matsushita, Y.; Kajii, Y.; Obi, K. *J. Phys. Chem.* **1992**, *96*, 6566–6570.
(12) Zimmerman, H. E.; Schuster, D. I. *J. Am. Chem. Soc.* **1962**, *84*, 4527–4540.
(13) Turro, N. J. *Modern Molecular Photochemistry*; University Science Books: Mill Valley, CA, 1991.
(14) Lukeman, M.; Xu, M. S.; Wan, P. *Chem Commun.* **2002**, *2*, 136–137.
(15) Mitchell, D.; Lukeman, M.; Lehnherr, D.; Wan, P. *Org. Lett.* **2005**, *7*, 3387–3389.
(16) Basarić, N.; Mitchell, D.; Wan, P. *Can. J. Chem.* **2007**, *85*, 561–571.
(17) Hou, Y. Y.; Huck, L. A.; Wan, P. *Photochem. Photobiol. Sci.* **2009**, *8*, 1408–1415.
(18) Huck, L. A.; Wan, P. *Org. Lett.* **2004**, *6*, 1797–1799.
(19) Mitchell, D. P. Doctoral dissertation, University of Victoria, 2008.
(20) Ramseier, M.; Senn, P.; Wirz, J. *J. Phy. Chem. A* **2003**, *107*, 3305–3315.
(21) Ljunggren, B. *Photodermatology* **1985**, *2*, 3–9.
(22) Przybilla, B.; Schwab-Przybilla, U.; Ruzicka, T.; Ring, J. *Photodermatology* **1987**, *4*, 73–78.
(23) Costanzo, L. L.; De Guidi, G.; Condorelli, G.; Cambria, A.; Fama, M. *Photochem. Photobiol.* **1989**, *50*, 359–365.
(24) Buntinx, G.; Poizat, O. *Laser Chem.* **1990**, *10*, 333–347.
(25) Bosca, F.; Carganico, G.; Castell, J. V.; Gomez-Lechon, M. J.; Hernandez, D.; Mauleon, D.; Martinez, A. L.; Miranda, M. A. *J. Photochem. Photobiol. B* **1995**, *31*, 133–138.
(26) Du, Y.; Xue, J. D.; Ma, C. S; Kwok, W. M.; Phillips, D. L. *J. Raman Spectrosc.* **2008**, *39*, 1518–1525.
(27) Du, Y.; Xue, J. D; Li, M. D.; Phillips, D. L. *J. Phys. Chem. A* **2009**, *113*, 3344–3352.
(28) Chuang, Y. P.; Xue, J. D.; Du, Y.; Li, M. D.; An, H. Y.; Phillips, D. L. *J. Phys. Chem. B* **2009**, *113*, 10530–10539.
(29) Du, Y.; Ma, C. S.; Kwok, W. M.; Xue, J. D.; Phillips, D. L. *J. Org. Chem.* **2007**, *72*, 7148–7156.
(30) Li, M. D.; Du, Y.; Chuang, Y. P.; Xue, J. D.; Phillips, D. L. *Phys. Chem. Chem. Phys.* **2010**, *12*, 4800–4808.
(31) Webb, S. P.; Yeh, S. W.; Phillips, L. A.; Tolbert, L. M.; Clark, J. H. *J. Am. Chem. Soc.* **1984**, *106*, 7286–7288.
(32) Webb, S. P.; Phillips, L. A.; Yeh, S. W.; Tolbert, L. M.; Clark, J. H. *J. Phys. Chem.* **1986**, *90*, 5154–5164.
(33) Schwartz, B. J.; A., P. L.; Harris, C. B. *J. Phys. Chem.* **1992**, *96*, 3591–3598.
(34) Toscano, J. P. *Adv. Photochem.* **2001**, *26*, 41–91.
(35) Toscano, J. P. In *Reviews of Reactive Intermediate Chemistry*; Platz, M. S.; Moss, R. A.; Jones, M., Jr., Eds.; John Wiley and Sons, Inc.: Hoboken, NJ, 2007; pp 183−206.
(36) Ma, C.; Kwok, W. M.; Chan, W. S.; Du, Y.; Kan, J. T. W.; Toy, P. H.; Phillips, D. L. *J. Am. Chem. Soc.* **2006**, *128*, 2558–2570.
(37) Lhiaubet, V.; Paillous, N.; Chouini-Lalanne, N. *Photochem. Photobiol.* **2001**, *74*, 670–678.
(38) Schwarz, H. A. *J. Chem. Educ.* **1981**, *58*, 101–105.
(39) Frisch, M. J.; Trucks, G. W.; Schlegel, H. B.; Scuseria, G. E.; Robb, M. A.; Cheeseman, J. R.; Montgomery, J. A., Jr.; Vreven, T.; Kudin, K. N.; Burant, J. C.; Millam, J. M.; Iyengar, S. S.; Tomasi, J.; Barone, V.; Mennucci, B.; Cossi, M.; Scalmani, G.; Rega, N.; Petersson, G. A.; Nakatsuji, H.; Hada, M.; Ehara, M.; Toyota, K.; Fukuda, R.; Hasegawa, J.; Ishida, M.; Nakajima, T.; Honda, Y.; Kitao, O.; Nakai, H.; Klene, M.; Li, X.; Knox, J. E.; Hratchian, H. P.; Cross, J. B.; Bakken, V.; Adamo, C.; Jaramillo, J.; Gomperts, R.; Stratmann, R. E.; Yazyev, O.; Austin, A. J.; Cammi, R.; Pomelli, C.; Ochterski, J. W.; Ayala, P. Y.; Morokuma, K.; Voth, G. A.; Salvador, P.; Dannenberg, J. J.; Zakrzewski, V. G.; Dapprich, S.; Daniels, A. D.; Strain, M. C.; Farkas, O.; Malick, D. K.; Rabuck, A. D.; Raghavachari, K.; Foresman, J. B.; Ortiz, J. V.; Cui, Q.; Baboul, A. G.; Clifford, S.; Cioslowski, J.; Stefanov, B. B.; Liu, G.; Liashenko, A.; Piskorz, P.; Komaromi, I.; Martin, R. L.; Fox, D. J.; Keith, T.; Al-Laham, M. A.; Peng, C. Y.; Nanayakkara, A.; Challacombe, M.; Gill, P. M. W.; Johnson, B.; Chen, W.; Wong, M. W.; Gonzalez, C.; Pople, J. A. *Gaussian 03, Revision C.02 ed.*; Gaussian, Inc.: Pittsburgh, PA, 2004.